



LAWRENCE  
LIVERMORE  
NATIONAL  
LABORATORY

# Analysis of snowflake divertor configurations for HL-2M

G. Y. Zheng, X. Q. Xu, D. D. Ryutov

March 11, 2014

Fusion Engineering and Design

## **Disclaimer**

---

This document was prepared as an account of work sponsored by an agency of the United States government. Neither the United States government nor Lawrence Livermore National Security, LLC, nor any of their employees makes any warranty, expressed or implied, or assumes any legal liability or responsibility for the accuracy, completeness, or usefulness of any information, apparatus, product, or process disclosed, or represents that its use would not infringe privately owned rights. Reference herein to any specific commercial product, process, or service by trade name, trademark, manufacturer, or otherwise does not necessarily constitute or imply its endorsement, recommendation, or favoring by the United States government or Lawrence Livermore National Security, LLC. The views and opinions of authors expressed herein do not necessarily state or reflect those of the United States government or Lawrence Livermore National Security, LLC, and shall not be used for advertising or product endorsement purposes.

# Magnetic configuration flexibility of snowflake divertor for HL-2M

G.Y.Zheng<sup>1,2</sup>, X.Q.Xu<sup>2</sup>, D.D.Ryutov<sup>2</sup>, Y.D. Pan<sup>1</sup> and T.Y.Xia<sup>3</sup>

<sup>1</sup>Southwestern Institute of Physics, Chengdu, People's Republic of China

<sup>2</sup>Lawrence Livermore National Laboratory, Livermore, CA 94550, USA

<sup>3</sup>Institute of Plasma Physics, Chinese Academy of Sciences, Hefei, People's Republic of China

## Abstract

HL-2M<sup>[1]</sup> is a tokamak device that is under construction. Based on the magnetic coils design of HL-2M, four kinds of divertor configurations are calculated by CORSICA code<sup>[2]</sup> with the same main plasma parameters, which are standard divertor, exact snowflake divertor, snowflake-plus divertor and snowflake-minus divertor configurations. The potential properties of these divertors are analyzed and presented in this paper: low poloidal field area around X-point, connection length from outside mid-plane to the primary X-point, target plate design and magnetic field shear. The results show that the snowflake configurations not only can reduce the heat load at divertor target plates, but also may improve the magneto-hydrodynamic stability by stronger magnetic shear at the edge. A new divertor configuration, named “tripod divertor”, is designed by adjusting the positions of the two X-points according to plasma parameters and magnetic coils current of HL-2M.

Key words: snowflake divertor, poloidal field, magnetic field shear, tripod divertor

PACS numbers: 52.55.Fa, 52.55.-s, 52.55.Rk

## 1 Introduction

Handling the high power and particle exhaust in fusion reactors based on standard divertor technologies is a challenging problem<sup>[3-5]</sup>. For DEMO study, the fusion power is about 5 times larger than that of ITER<sup>[6]</sup>, but the tolerable heat load on the divertor is below 10MW/m<sup>2</sup> which is one of the design targets for DEMO steady-state operation. How to handle such large exhaust power in SOL/divertor regions is one of the key issues in validating the design of DEMO<sup>[7]</sup>. For standard divertor, a high fraction of the heating power has to be radiated in the core or SOL region to make the peak heat load under 10MW/m<sup>2</sup>. But the impurity seeded at the boundary will be partly transported into the core plasma zone, and cause the core energy confinement to decline. This, in turn, will make it difficult to attain high normalized plasma beta which is needed for the commercial fusion reactor operation with high fusion power density<sup>[8]</sup>. ~~How to reduce the divertor heat load by purely redesign of divertor magnetic field geometry has been considered, and a few promising divertor concepts are proposed~~One of approaches to solution of this problem is based on employing novel magnetic field geometries, such as Cusp divertor<sup>[9]</sup>, X-divertor<sup>[10]</sup>, Super-X divertor<sup>[11]</sup> and snowflake divertor<sup>[12]</sup>. Cusp divertor and X-divertor considerably enhance the divertor thermal capacity through a flaring of the field lines near the divertor target plates. Super-X divertor moves the divertor plates to the largest possible radius  $R_{div}$  inside toroidal field

(TF) coils to increase the plasma-wetted area and magnetic connection length from the plasma by largest  $R_{div}$ , and broaden the magnetic flux at largest  $R_{div}$  to decrease the parallel heat flux and plasma temperature at divertor plate. The snowflake divertor creates the second order null of the poloidal magnetic field in the X-point zone, not a first order as in standard divertor, and the separatrix in the vicinity of the null point splits the poloidal plane into six sectors.

HL-2M is a new medium-sized copper-conductor tokamak device being constructed to be put into operation in the near future<sup>[1]</sup>. It aims at the experiments to study the high performance plasma physics and engineering toward ITER and even a fusion reactor. In order to enhance the flexibility and controllability of experiments to achieve high plasma performance, HL-2M is designed with a demountable TF coils; poloidal field (PF) coils will be placed inside the TF coils. From engineering point of view, when PF coils get close to the core plasma, it will increase their feedback control ability for high plasma performance, such as larger elongation, higher plasma pressure, etc. Moreover, it will reduce the PF coils current to generate a second X-point. So it provides HL-2M with the ability to generate a few kinds-types of advanced divertor configuration, such as exact snowflake divertor, snowflake-plus divertor, etc. These advanced divertor configurations can be explored in HL-2M experimental research project. The total design heating power of HL-2M will be 32MW, the heat load at target can be roughly compared by  $P/R$ , where  $P$  is the heating power flows into SOL zone and  $R$  is the major radius.  $P/R$  is 18 MW/m for HL-2M, which is higher than that of ITER (16MW/m). This means HL-2M will face greater challenges than ITER for divertor design to reduce the peak heat load to less than 10MW/m<sup>2</sup>, or even lower value. From another perspective, HL-2M will have the ability to operate with high plasma quality and advanced divertor with 32MW heating power. This means HL-2M will be an excellent platform to test the engineering and physics issues related to fusion reactor, and will provide important data for China Fusion Engineering and Testing Reactor (CFETR) or even for DEMO advanced divertor design.

Based on the PF coils design, a few of different divertor configurations are analyzed by CORSICA equilibrium code under the same key parameters. The figures of merit for these divertors are calculated and compared in this paper, which are the magnetic shears, the area of low poloidal magnetic field  $B_p$  around X-point and the connection length from outer mid-plane to the primary X-point. The results of these properties may help us to improve our advanced divertor design in more detail. At last, a new divertor configuration called tripod divertor is investigated and presented.

## 2 HL-2M snowflake divertor configurations

The standard divertor designs have been carried out and optimized in Southwestern Institute of Physics (SWIP). According to the design parameters, plasma current is  $I_p = 2.0MA$ , poloidal beta is  $\beta_p = 0.6$  and internal inductance is  $l_i = 1.2$ . A standard divertor configuration is calculated using CORSICA equilibrium code with a free-boundary Grad-Shafranov solver. The configuration and positions of PF coils of HL-2M are shown in figure 1, where major radius  $R = 1.78m$ , minor radius  $a = 0.62m$ , plasma current  $I_p = 2.0MA$  and elongation  $k_{95} = 1.6$ . The plasma pressure and current profiles used for CORSICA calculation are shown in figure 2. The H-mode pressure

edge pedestal and bootstrap current inside the separatrix in boundary zone estimated by HL-2M operation scenarios, which are included for equilibrium calculations. For the standard divertor configuration, the PF5/L and PF6/L coils are used as divertor coils to generate X-point and control the configuration. Because PF5/L and PF6/L coils are too close to generate two separate X-points, the standard divertor configuration typically has only one X-point of the poloidal field ( $B_p$ ). In order to have a second order X-point nearby, it is better to have a PF coil between the two divertor coils, which helps to reduce the current of two divertor coils and enhance the control capability for the two X-points, especially the second X-point. So based on HL-2M PF coils design, we choose PF4/L and PF6/L as divertor coils to generate two separate X-points, and use PF5/L to adjust the position of the two X-points. When two X-points get close enough to achieve  $B_p$  null being of second order, the configuration becomes of hexagonal geometry, ~~being and is~~ named “as snowflake divertor”. By adjusting currents in these three PF coils, the position of the X-points can be changed to satisfy the physical and engineering design requirement, such as increase the magnetic flux expansion at divertor target to reduce the heat load at target. By the standard definitions of snowflake divertor<sup>[12,13]</sup>, HL-2M can achieve the exact snowflake, snowflake-plus and snowflake-minus divertor configurations, which are shown in figure 3. The four divertor configurations will allow us to optimize the divertor design while keeping the same main design parameters ( $R = 1.78m, a = 0.62m, I_p = 2.0MA, k_{95} = 1.6, q_{95} = 3.0$  and  $\beta_p = 0.6$ ) and current and pressure profiles.

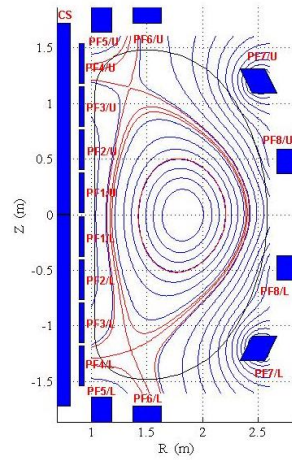


Figure 1. Standard divertor configuration. The filled blue boxes show the position of PF coils with the corresponding numbers. The long blue boxes at the far left represent the central solenoid (CS) coil.

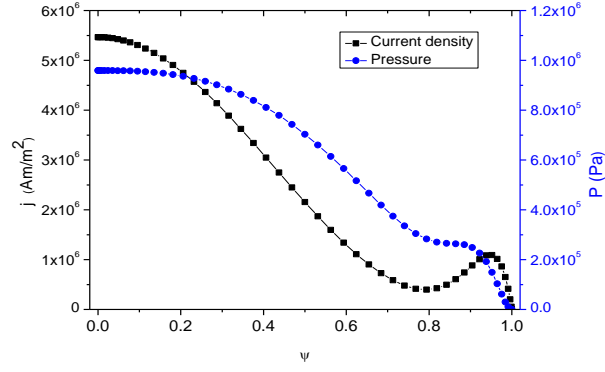


Figure 2. The radial profiles of current and pressure.

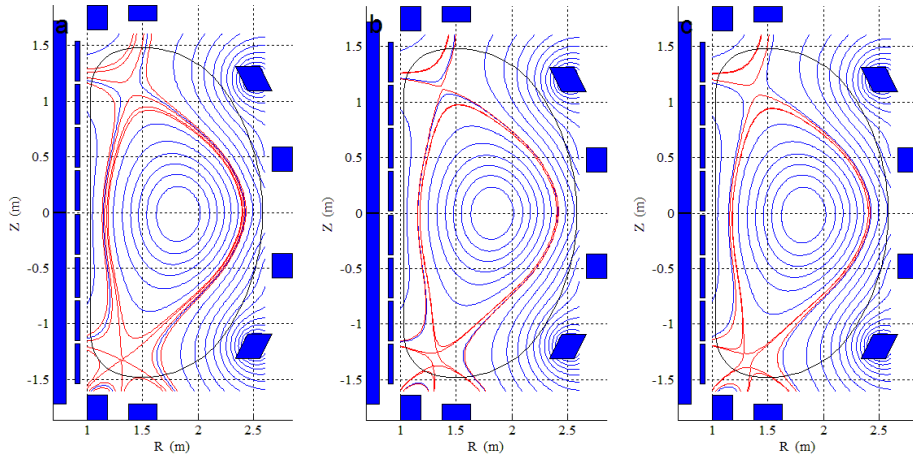


Figure 3. Snowflake divertor configurations: a) exact snowflake divertor configuration, b) snowflake-plus divertor configuration, c) snowflake-minus divertor configuration.

### 3 Low $B_p$ area

As the  $B_p$  null is of second order for snowflake divertor configuration, it yields a larger area of low  $B_p$  zone surrounding the two X-points<sup>[13]</sup>. For quantitative analysis of the effect of poloidal field  $B_p$  on different divertor configurations around the X-point, a set of HL-2M ~~tokamak~~ tokamak equilibrium configurations shown in figure 3 are compared. The area for small  $B_p$  around the X-point is measured by  $F_p$ , which is  $F_p = B_p / B_{p-mid}$ ;  $B_{p-mid}$  is the poloidal field strength at the outside mid-plane. The  $F_p$  value around X-points for four divertor configurations is shown in figure 4. Since the  $B_{p-mid}$  value is the same for the four divertor configurations, small  $F_p$  values mean low  $B_p$  around X-point, and  $F_p$  decreases when approaching the X-points.  $F_p < 0.1$  is considered as a low field zone. Snowflake divertors have a large low  $B_p$  zone surrounding the two X-points, and the shape of the low  $B_p$  area will change according to the position of the two X-points. As shown in figure 4, the area of low  $B_p$  zone for three snowflake divertor configurations is almost the same and is three times larger than that for standard divertor configuration when  $F_p < 0.1$ . The area of standard divertor shrinks faster than that of snowflake with  $F_p$  decrease. When  $F_p < 0.03$ , the area of standard divertor become very small, which is

less than 10% of that for snowflake divertor.

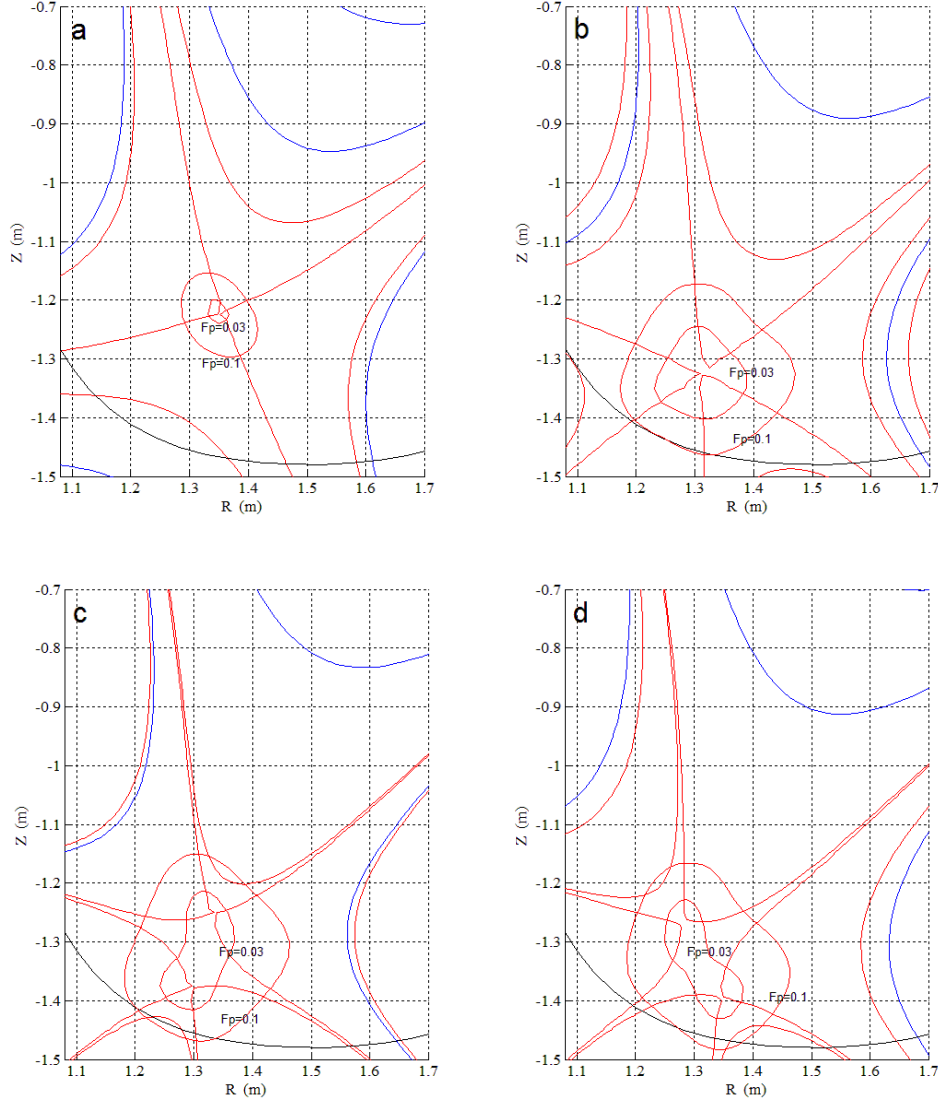


Figure 4. Low  $B_p$  area around X-points; a) standard divertor configuration, b) exact snowflake divertor configuration, c) snowflake-plus divertor configuration, d) snowflake-minus divertor configuration.

As the particles and energy flow into low  $B_p$  zone along the magnetic field line, the ratio of the plasma pressure to the pressure of the poloidal magnetic field,  $\beta_p$  will increase rapidly and will become 100 times to 1000 times larger than that at outside mid-plane with  $F_p = 0.1$  and  $F_p = 0.03$ . So for snowflake divertor, it will form a larger zone with high local  $\beta_p$  that is expected to lead to the onset of fast convective heat transport<sup>[14-17]</sup>. Fast convective heat transport around the low  $B_p$  can increase power sharing among divertor legs and broaden the heat load profile on divertor target plates, especially during an ELM bursts. HL-2M snowflake divertor configuration design should be able to take the advantage of the large convective heat transport to optimize the low  $B_p$  area round the two X-points to reducing the heat load at target with different operation parameters.

## 4 Connection length

The connection length is a measure of the residence time of the particles in the SOL, which is defined as the length of a magnetic field line from the ~~middle-mid~~-plane to the target. Increasing the connection length will lead to a relatively larger divertor volume available for radiation and a significant broadening of the heat flux profile on the target due to cross field heat and particle transport. Although the plasma, due to the anomalous cross-field diffusion, may not follow the flux surfaces on its way to the target, the connection length remains a convenient parameter that allows, in particular, to evaluate the magnitude of the anomalous transport needed for the power sharing between multiple divertor legs. So Generally, increasing-increased connection length is one of feasible methods should be helpful to-for mitigate-mitigating the heat load at target, especially during edge-localized modes (ELMs). As shown above, snowflake divertor has larger low  $B_p$  area than that in a standard divertor configuration, which results in a longer connection length. Here the connection length for a segment of magnetic line is calculated by  $B/B_p * L_{pol}$ ,  $B$  is the magnetic field strength,  $L_{pol}$  is the poloidal length of the segment. Connection length is calculated from the outside mid-plane to the position which is the closest to the primary X-point along the magnetic field line. Figure 5 shows the radial profiles of connection length at outside mid-plane for various divertor configurations: standard divertor (black), snowflake-plus (red), and snowflake-minus (blue). Owing to the large area of low field zone, the snowflake-plus and snowflake-minus configurations have almost the same connection length at the positions close to separatrix, which is 50%-80% longer than that of standard divertor. Because of the peak heat load is typically near separatrix, so longer connection length will help to mitigate the peak heat load at target for snowflake divertor configurations.

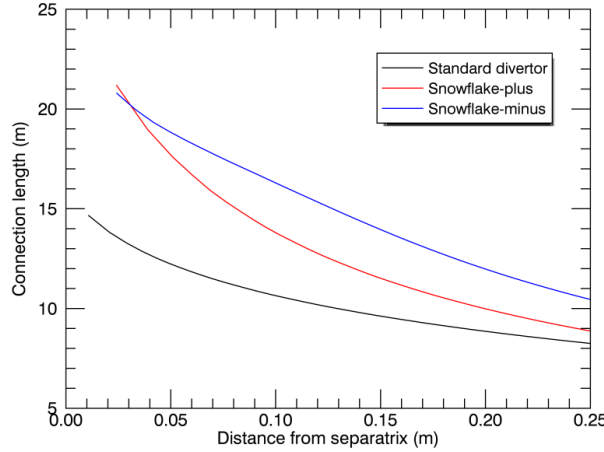


Figure 5. The radial profiles of connection length at outside mid-plane for various divertor configurations: standard divertor (black), snowflake-plus (red), and snowflake-minus (blue).

## 5 Target plate

If the target plate is normal to the poloidal field vector at the strike point, the field lines form an



angle  $\gamma \approx B_p/B_t = F_t$  with this plate. One can further reduce the intersection angle by tilting the plate in the poloidal plane, so that the poloidal field will form some angle  $\alpha < \pi/2$  with the plate. In this case the field lines will intersect the plate at an angle  $\gamma \approx F_t \sin \alpha$ . Smaller  $\alpha$  means a larger wetted area, so that decreasing  $\alpha$  seems to be an efficient way of decreasing the heat flux. However, engineering constraints may limit the value of  $\gamma$  from below<sup>[11,13,18]</sup>, by some minimum value  $\gamma_{min}$  determined by the achievable flatness of the plate. If  $\gamma_{min}$  is too small, the shadows and hot spots will-may appear on the plate, leading to uncontrolled damage. Typically,  $\gamma_{min}$  is assumed to be 1/50 of a radian (roughly 1 degree). A corollary is that it is not particularly desirable to make the parameter  $F_t$  at the strike point less than 1/50. The  $F_t$  value around X-point for four kinds divertor configurations are calculated and shown in figure 6. Two X-points are included in the  $F_t < 1/50$  zone for snowflake divertor, and the target should not be placed between two X-points, even if  $\alpha = \pi/2$ . So we can place the target between two X-points by increasing the  $F_t$  value with larger two X-point distance or place the target below the second X-point with  $F_t > 1/50$ , then optimize the target geometry with  $F_t$  value to increase the wetted area and particles recycling.

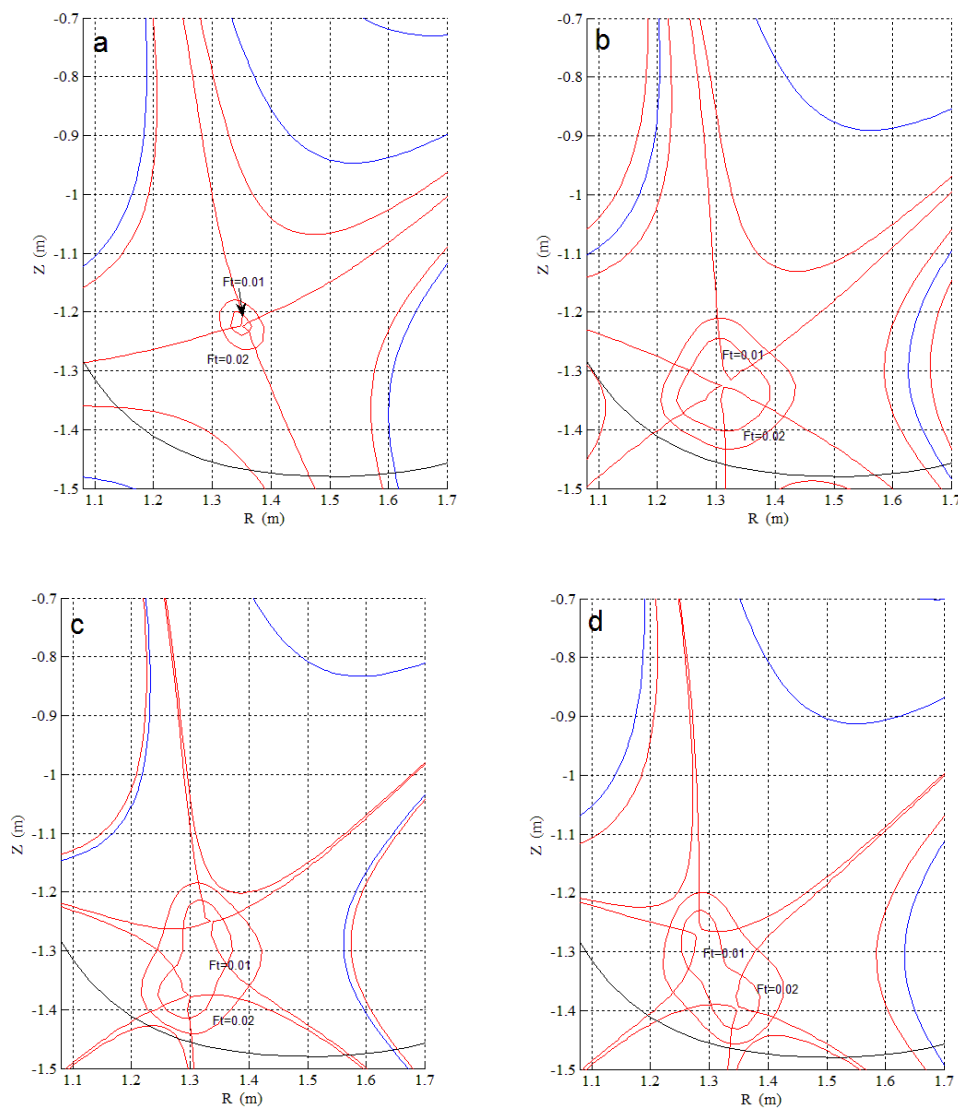


Figure 6.  $F_t$  value around X-point; a) standard divertor configuration, b) exact snowflake divertor configuration, c) snowflake-plus divertor configuration, d) snowflake-minus divertor configuration.

## 6 Magnetic shear

Stronger shearing of the magnetic field generally leads to stronger stabilization of ideal MHD modes. Therefore we expect to have a stronger magnetic shear to improve the MHD stability in the edge, in particular during ELMs. Snowflake divertor has a larger low  $B_p$  area around the X-points compared to the standard divertor, which results in stronger magnetic shear around the X-point, and even change the magnetic shear near pedestal zone<sup>[17,19,20]</sup>. Based on a set of HL-2M tokamak equilibrium configurations shown above,  ~~$d_x = 15\text{cm}$~~  with the distance  $d_x$  between the two X-points  $d_x = 15\text{cm}$  for both snowflake-plus and snowflake-minus,  ~~$d_x$  is the distance between the two X-points.~~ The safety factor ( $q$ ) profiles and integrated magnetic shear value profiles  $S = \frac{r}{q} \frac{dq}{dr}$  are shown in figure 7 and figure 8, which show that snowflake divertor configurations have larger  $q$  value and integrated magnetic shear value than standard divertor configuration at boundary zone with the same  $q_{95} = 3.0$ , especially the exact snowflake divertor and snowflake-minus divertor configurations.

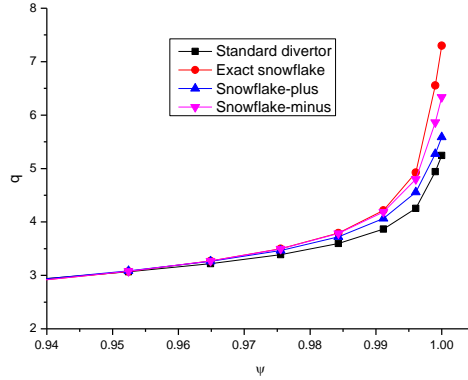


Figure 7.  $q$  value.

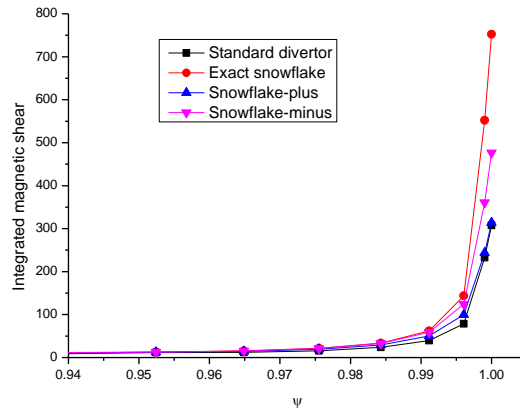


Figure 8. Integrated magnetic shear value.

The poloidal profiles of the local magnetic shear inside the separatrix also is investigated, the local magnetic shear  $s$  is:  $s = \frac{RB_p}{B_t} \frac{dv}{dr}$ ,  $v = \frac{rB_t}{RB_p}$ , where  $v(\Psi, \theta)$  is local pitch and its flux surface average yields safety factor  $q(\Psi) = \langle v(\Psi, \theta) \rangle_{\text{sur}}$ .  $\Psi$  is normalized poloidal flux changing from 0 at the magnetic axis to 1 at separatrix. The maximum pressure gradient is at  $\Psi = 0.97$  for the four divertor configurations. The poloidal profiles of the local magnetic shear at  $\Psi = 0.97$  is shown in figure 9. Along the poloidal direction, the local magnetic shear of snowflake divertor around the primary X-point zone is much larger than that of standard divertor, which is expected to have stronger stabilization effect on ideal MHD modes. **The difference of local magnetic shear at  $\Psi$  less than 0.95 between snowflake and standard divertor will become smaller, that means that the snowflake divertor only has significant effects on the local magnetic shear near the bottom of pedestal zone with  $0.95 < \Psi < 1.0$ .** Furthermore, the three snowflake divertor configurations shown in figure 4 have almost the same local magnetic shear, and the difference of local magnetic field around primary X-point zone ~~will becomes~~ obvious ~~by only~~ when  $0.99 < \Psi < 1.0$ . The local magnetic ~~field-shear~~ at outside mid-plane ~~are-is~~ shown in figure 10. At outside mid-plane, local magnetic shear of exact snowflake divertor is about 10% larger than that of standard divertor at  $0.95 < \Psi < 1.0$ , which may lead to reduce growth rate and narrower radial mode structures for peeling-ballooning mode<sup>[19,20]</sup>. A two-fluid three-field MHD model has been used to study the peeling-ballooning (P-B) stability properties in snowflake-plus and standard divertor configurations for DIII-D configuration<sup>[19]</sup>. The results show that the larger magnetic shear around the X-point in snowflake-plus divertor suppresses the P-B modes in divertor zone, while the smaller magnetic shear at outer mid-plane causes higher growth rate and broader radial mode structure. Therefore the sensitivity of the linear behaviors of P-B modes on the small changes of the local magnetic shear at the outer mid-plane imposes important design constraints of advanced divertors on the tokamak. The second X-point of snowflake-minus divertor is more close to the outside mid-plane, which may cause its local magnetic shear in the mid-plane increases fast at  $0.95 < \Psi < 1.0$ .

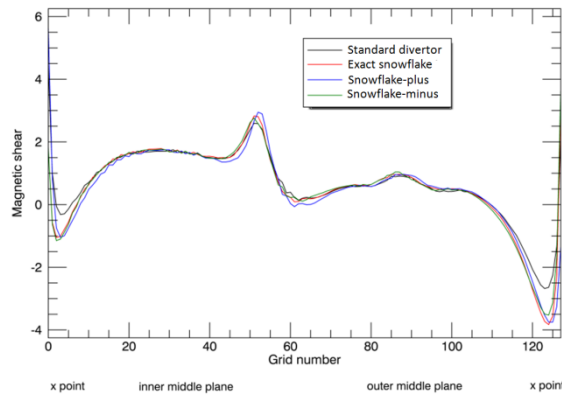


Figure 9. Local magnetic shear profiles at  $\Psi = 0.97$ .

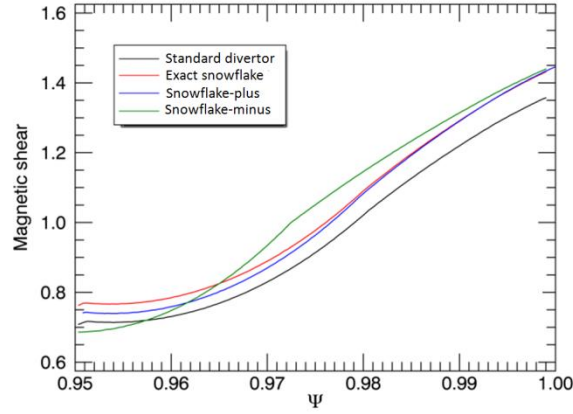


Figure 10. The radial profiles of the local magnetic ~~field-shear~~ at outside mid-plane.

ELMs are ~~caused by~~ ideal MHD peeling-ballooning instability driven by edge gradients and stabilized by the shear. So the increased shear of HL-2M snowflake divertor may have important implications for ELMs. For stronger shear one can maintain an ELM-free regime with larger edge gradients, which means HL-2M can operate under higher edge pedestal pressure and better overall performance with snowflake divertor configuration.

## 7 Distance between two X-points

HL-2M magnetic field coils design shows that the poloidal magnetic field from central solenoid (CS) coil will partly enter the plasma zone, and will affect the configuration by forcing the configuration to move outward and X-point position to move up. By taking the advantage of the poloidal magnetic field from CS coil and adjusting the PF coils current values, the configurations of different plasma current with the same current and pressure profiles are calculated and shown in figure 11. When  $I_p = 2MA$ , it is a snowflake-minus divertor configuration ~~that~~ has the large low  $B_p$  area with  $F_p \leq 0.1$ , which contains the two X-points with  $d_x = 15cm$ . But if  $I_p = 1.5MA$ , the primary X-point is forced to move up and generated the second X-point with  $d_x = 30cm$ , and the areas with  $F_p \leq 0.1$  zone are just around the two X-points with ~~small-an~~ area which is much smaller than the case  $I_p = 2MA$ . ~~The parameter  $d_x$  will be increasing increase-with  $I_p$  reduces decreasing~~ for HL-2M. At large distance between the two X-points, the effect of the second X-point on the field structure at the primary one decreases and the configuration eventually loses the features of a snowflake divertor, becomes just that of the two separate X-points. On the other hand, the emerging configuration is different from a prototypical X-divertor<sup>[10]</sup> or conceptually similar cusp divertor<sup>[9]</sup> that relies on the use of specially arranged coils near the strike point. So, we suggest to call a configuration with a long divertor leg and three outgoing branches of the separatrix a “tripod configuration”.

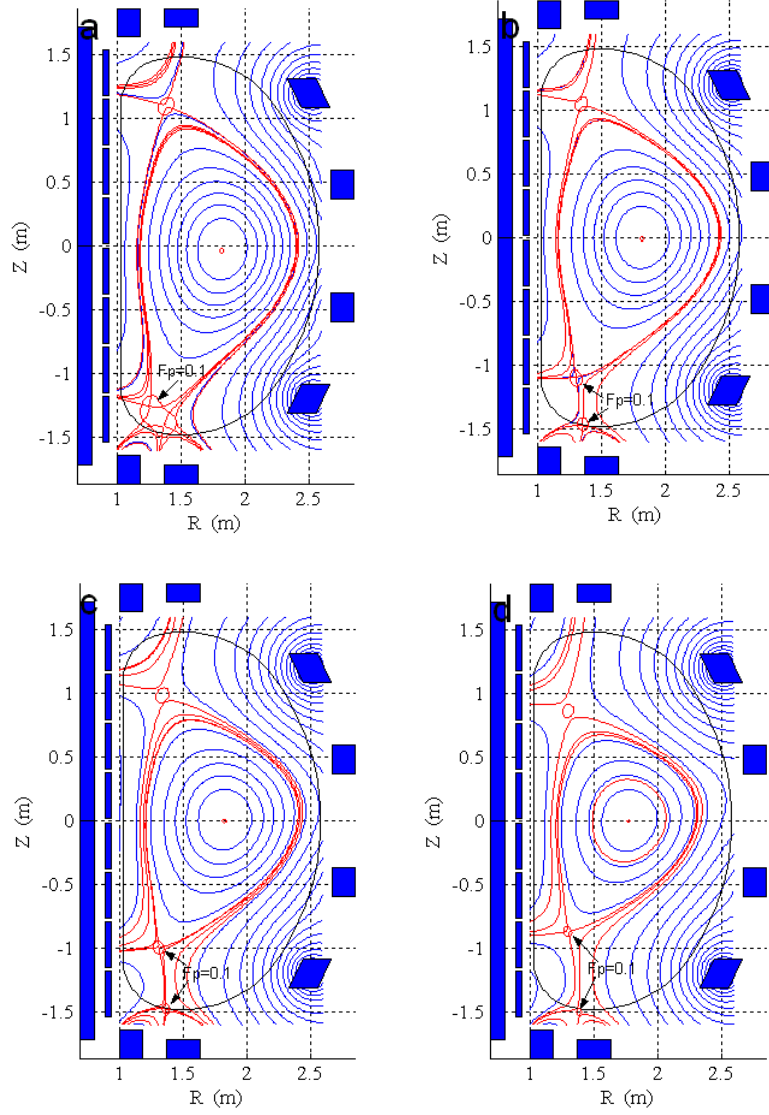


Figure 11. The configurations of different plasma current; a)  $I_p = 2MA$  snowflake-minus divertor configuration, b)  $I_p = 1.5MA$ , c)  $I_p = 1.2MA$ , d)  $I_p = 0.9MA$ . We call configurations b-d the “tripod” configurations; they have also some attributes of a cusp and X-divertor configurations.

## 8 Discussion

Based on the four different divertor configurations of HL-2M with the same main plasma parameters calculated by CORSICA code, potential properties of these divertors are analyzed. The results show that snowflake divertor configurations have larger low  $B_p$  area around the primary X-point ~~in-at~~ the edge of snowflake divertor, it may reduce the heat load at target plate by fast convective heat transport around the low  $B_p$  zone with higher  $\beta_p$ , larger plasma-wetted area and longer connection length to broaden or share the heat load profile at targets, especially when an ELM event happens. But the maximum wetted area will be limited with engineering constrain by  $\gamma_{min}$ , so we should optimize target geometry according to the  $F_t$  value by adjusting the position of the two X-points. The stronger magnetic shear of HL-2M snowflake divertors also may be beneficial for the magneto-hydrodynamic instabilities in the edge to improve core plasma

confinements. At last, a new divertor configuration called tripod divertor is generated by adjusting the magnetic coil currents, which has a longer divertor leg and magnetic connection length with larger distance between the two X-points, and a broadened magnetic flux with the second X-point near the divertor target plate.

### Acknowledgements

The authors wish to acknowledge Drs. R.H. Bulmer, M. V. Umansky, and G. Q. Li for their valuable suggestions, advice and timely help for using CORSICA code during this research. Many thanks in particular to Drs. Y. Liu and X. R. Duan for their support and encouragement for US-China international collaboration project. This work was supported by Chinese ITER Plan Project Foundation (Grant Nos. 2013GB113001), National Science Foundation of China (grant Nos. 11275061 and 11175058), and by LLNL for USDOE under DE-AC52-07NA27344. LLNL-JRNL-651522.

### References

- [1] Q. Li, Proceedings 25th Symposium on Fusion Engineering, TPO-113 , (2013).
- [2] L. D. Pearlstein, et al., Proceedings 28th EPS Conference, P5.034, (2001).
- [3] D. J. Campbell, Phys. Plasmas 8, 2041 (2001).
- [4] A. S. Kukushkin, et al., Fusion Eng. Des. 65, 355 (2003).
- [5] V. Mukhovatov, et al., Plasma Phys. Controlled Fusion 45, A235 (2003).
- [6] K. M. Feng et al., Fusion Eng. Design 84, 2109 (2009).
- [7] H. Kawashima, et al., Nucl. Fusion 49 (2009) 065007.
- [8] M. Kotschenreuther, et al., Nucl. Fusion 50, 035003(2010).
- [9] H. Takase, Journal of the Physical Society of Japan 70, 609(2001).
- [10] M. Kotschenreuther, et al., Phys. Plasmas 14, 072502 (2007).
- [11] P. M. Valanju, et al., Phys. Plasmas 16, 056110 (2009).
- [12] D. D. Ryutov, Phys. Plasmas 14, 064502 (2007).
- [13] D. D. Ryutov, Phys. Plasmas 15, 092501(2008).
- [14] D. D. Ryutov, et al., Contrib. Plasma Phys.52, No. 5-6, 539543, (2012).
- [15] D. D. Ryutov, et al., Plasma Phys. Controlled Fusion 52 124050, (2012).
- [16] W. A. J. Vijvers, et al., Nucl. Fusion 54 [023009](#), (2014).
- [17] D. D. Ryutov, et al., Proceedings of 24nd IAEA Fusion Energy Conference, TH/P4-18 , (2012).
- [18] A. S. Kukushkin, private communication to D. D. Ryutov (2007).
- [19] J. F. Ma, et al., Nucl. Fusion 54 (2014).
- [20] M. V. Umansky, et al., Contrib. Plasma Phys. 50, No. 3-5, 350-355 (2010).